Lab on a Chip

PAPER

View Article Online
View Journal

Cite this: DOI: 10.1039/c6lc00391e

Droplet immobilization within a polymeric organogel improves lipid bilayer durability and portability†

Guru A. Venkatesan and Stephen A. Sarles*

Received 22nd March 2016,
Accepted 28th April 2016

DOI: 10.1039/c6lc00391e

www.rsc.org/loc

The droplet interface bilayer (DIB) is a promising technique for assembling lipid membrane-based materials and devices using water droplets in oil, but it has largely been limited to laboratory environments due to its liquid construction. With a vision to transform this lab-based technique into a more-durable embodiment, we investigate the use of a polymer-based organogel to encapsulate DIBs within a more-solid material matrix to improve their handling and portability. Specifically, a temperature-sensitive organogel formed from hexadecane and poly[styrene-*b*-(ethylene-co-butylene)-*b*-styrene] (SEBS) triblock copolymer is used to replace the liquid solvent that surrounds the lipid-coated droplets to establish a novel liquid-in-gel DIB system. Through specific capacitance measurements and single-channel recordings of the pore forming peptide alamethicin, we verify that the structural and functional membrane properties are retained when DIBs are assembled within SEBS organogel. In addition, we demonstrate that organogel encapsulation offers improved handling of droplets and yields DIBs with a near 3× higher bilayer durability, as quantified by the lateral acceleration required to rupture the membrane, compared to liquid-in-liquid DIBs in oil. This encapsulated DIB system provides a barrier against contamination from the environment and offers a new material platform for supporting multilayered DIB-based devices as well as other digital microfluidic systems that feature water droplets in oil.

Introduction

Biomimetic soft materials featuring artificial cell membranes that imitate the properties and functionalities of those found in living organisms are being developed from nanoscale materials, such as phospholipids and natural or synthetic biomolecules. Over the last few decades, numerous techniques have been developed to construct, study, and utilize the two-dimensional lipid bilayer structure found ubiquitously in cells for the purpose of achieving a biomimetic platform capable of selective transport and biomolecule-mediated sensing and energy conversion.[1–3]

The droplet interface bilayer (DIB) is one of the newer techniques employed to construct synthetic lipid bilayers between lipid-coated water droplets connected in oil.[4,5] Engineered applications of single- and multi-membrane DIB networks range from the development of electrical rectifier circuits,[6] energy conversion platforms,[7] 3D-printed tissues capable of mechanical actuation,[8] bioinspired sensors,[9] and for use in the study of selective transport of ions and molecules.[10] A light sensing DIB network was also demonstrated by using the light sensitive channel, bacteriorhodopsin.[7] The DIB platform has also been implemented for studying the electro-physical activation and characterization of various transmembrane peptides and proteins such as alamethicin and α-hemolysin.[11,12] Recently, mechanical[13] and chemical[14] activation of MscL channels from *E. coli* were demonstrated by two independent groups using the DIB platform. These various uses highlight several advantages of DIBs, including their easy assembly and rearrangement, the ability to control both droplet and bilayer compositions, and a wide-range working temperature.[15] Another unique advantage of the DIB technique is its scalability in number and length scale: a single DIB can be assembled between two droplets, while many DIBs are formed by adjoining many droplets in 2 and 3 dimensions.[16] Additionally, DIBs can be formed across a wide range of length scales, from micron-sized droplets to mm-sized droplets.[8,17]

These attractive properties thus motivate the use of DIBs in the development of new types of multifunctional, membrane-based materials that employ the functionalities of a wide range of membrane-bound biomolecules for applications such as sensing, energy conversion, information and energy storage, color change, and actuation. However, due to

Mechanical, Aerospace, and Biomedical Engineering, University of Tennessee, 1512 Middle Drive, 414 Dougherty Engineering Building, Knoxville, TN 37996, USA. E-mail: ssarles@utk.edu

† Electronic supplementary information (ESI) available. See DOI: 10.1039/c6lc00391e

the nature of the liquid environment used to construct DIBs, DIB portability is highly limited, requiring delicate handling. This limitation is even greater for large droplet arrays in oil, since many paired droplets have greater total inertia in the oil and multiple membrane connections must be preserved to maintain a desired functionality. Conventional DIBs, referred to from hereon as the *liquid-in-liquid* system, require two liquid phases that are contained within a solid substrate. The liquid phases consist of an organic solvent (*i.e.* oil) comprising the bulk phase and aqueous electrolyte solutions that comprise the droplets. Placing these two fluids in an unsealed substrate (*i.e.* as is often the practice for laboratory-based experiments[18]) makes the system prone to spillage, leakage and contamination.

Previous attempts to make synthetic lipid bilayers more durable and portable include modifying the bilayer formation procedure or the use of a substrate designed to support the bilayer embodiment. Jeon *et al.* demonstrated a platform in which the bilayer precursors (aqueous droplets in organic phase) are frozen until their usage, allowing for increased portability and storage prior to membrane assembly.[19,20] Our attempts (unpublished) to freeze DIBs formed in hexadecane resulted in bilayer rupturing at 18 °C, the freezing point of hexadecane. Sarles *et al.* designed a closed PMMA/PDMS containment with integrated wire-type electrodes designed to hold and electrically interrogate a conventional DIB.[21] With this design, the DIB did not rupture or disassemble during simple handling such as moving, shaking and inverting, and an increase in the overall durability was reported. Yet, reconfiguring or refreshing a DIB within this substrate required complete disassembly of the multiple containment components. Another successful demonstration of improving the portability of planar lipid bilayers involved both substrate design and portable electronics: open-style droplet chambers separated by a porous, parylene film was used to form in parallel multiple planar lipid bilayers between droplets across the pores in the dividing film. This embodiment was accompanied by a handheld patch clamp amplifier from Tecella, which allowed for measurements of transmembrane bilayer currents in an outdoor environment.[22] While this system demonstrated portability of bilayer recordings, the authors did not validate whether bilayers formed in this substrate are portable or durable after assembly. Thus, a convenient and robust DIB platform that significantly improves the portability and durability without compromising the basic functionalities of a lipid bilayer is still needed.

In this article and for the first time to our knowledge, we study the use of a phase-changing poly[styrene-*b*-(ethylene-co-butylene)-*b*-styrene] (SEBS) organogel that solidifies from a molten liquid to a soft elastic gel at ~40 °C for developing a novel *liquid-in-gel* encapsulated DIB system that has improved portability and durability as compared to DIB systems that have been studied thus far. This temperature-sensitive organogel material is made by dissolving SEBS, a tri-block copolymer and thermoplastic elastomer, in hexadecane and heating the mixture to >40 °C; we use this molten mixture to replace the bulk organic phase that surrounds the lipid-coated aqueous droplets. To properly examine this substitution, we perform experiments on DIBs formed in the presence and absence of SEBS at both 50 °C and near room temperature to confirm that both lipid monolayer self-assembly and bilayer thinning between droplets are unobstructed by the presence of SEBS polymer molecules in the oil. We also record alamethicin ion channel gating in liquid-in-gel DIBs to demonstrate that the basic structural and functional properties of the lipid bilayer are retained, and we demonstrate that droplet encapsulation using organogel successively holds droplets in place and cushions them during accelerations, thereby achieving increased DIB durability and portability.

Methods and materials

Materials preparation

SEBS is purchased in powder form from Kraton (G-1650E; 10 kg mol^{-1}) and used without further purification. 10 mg ml^{-1} (1 mM) SEBS/hexadecane solution is prepared in a glass beaker by mixing appropriate amounts of SEBS and hexadecane, followed by heating the mixture to 100 °C until SEBS completely dissolves to produce a transparent solution. Following dissolution at 100 °C, the mixture is cooled and stored for up to 3 weeks at room temperature (RT, 25–28 °C). Molten organogel is obtained by reheating the organogel to 50 °C.

Aqueous liposome solution is prepared by a standard extrusion method as described in the ESI.† DPhPC phospholipids are purchased in powder form from Avanti Polar Lipids and used without further purification.[23] A pH-buffered electrolyte solution made up of 10 mM MOPS, 100 mM NaCl, pH 7.0 is used in the preparation the 2 mg ml^{-1} liposome solution. Alamethicin peptides purchased in powder form (A.G. Scientific) are dissolved in ethanol at 10 mg ml^{-1} and stored at −20 °C. Alamethicin stock solution is then diluted in liposome solution to yield a final concentration of 1 μM.

Experimental procedures

Liquid-in-liquid DIB formation. As shown in Fig. 1A, an open PMMA (polymethyl methacrylate)) or PDMS (polydimethylsiloxane) substrate with an open reservoir (1.5 cm deep) is filled with about 250 μl of hexadecane. 200–500 nl aqueous droplets containing DPhPC liposomes are then pipetted separately into the droplet compartment. After 3–5 minutes mandatory incubation time for monolayer assembly, droplets are brought into contact by gently pushing the droplets together using a pipette.[24] Upon contact, a DIB forms at the interface as excess solvent is spontaneously excluded from between the droplets.[25]

Liquid-in-gel DIB formation. In addition to the above-mentioned setup required for forming conventional DIB, a heating module consisting of a heating pad and a thermocouple are used to assemble organogel-encapsulated DIBs. A 30 mm × 30 mm resistive heating element (Omega, KHLV-101/10) is placed underneath a PMMA or PDMS substrate

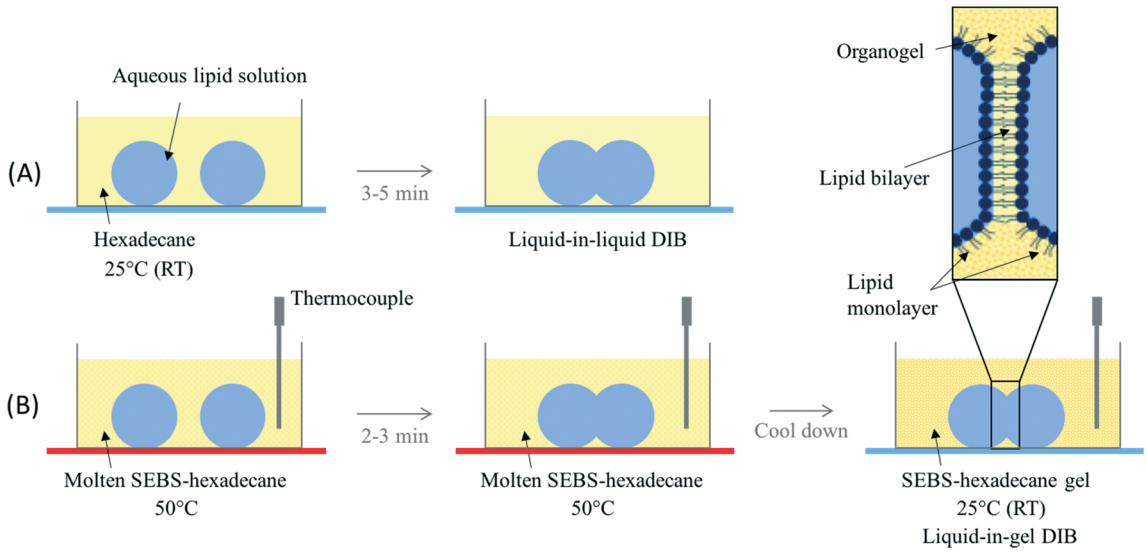

Fig. 1 Procedure for assembling a single DIB using: A) the liquid-in-liquid method, and B) the liquid-in-gel method.

and connected to a BK Precision 1788 digital power supply. The tip of a thermocouple (Omega, P/N:JMTSS-020 U-6)) probe is placed under the bulk solvent, adjacent to the aqueous droplets as shown in Fig. 1B. This allows close monitoring of the temperature of the external phase that surrounds the droplets. First, about 250 μl of molten SEBS/hexadecane solution is dispensed into the droplet compartment and the heater is turned on such that the temperature in the droplet compartment reaches 50 °C. At this temperature, the SEBS/hexadecane mixture remains in the molten phase with a viscosity of ~16 mPa s. In comparison, hexadecane and AR20 silicone oil (Sigma Aldrich), which have both been used as the oil phase for DIB formation at room temperature, have viscosities of 3 mPa s and 20 mPa s, respectively. 200–500 nl aqueous droplets are then pipetted into the substrate and are brought together after 2–3 minutes to form a DIB. Once the bilayer is formed, the heater is turned off to passively cool (~2 °C min^{-1} maximum cooling rate) the system to room temperature. The molten SEBS/hexadecane mixture starts to gelate upon cooling below 40 °C where it turns into a weak gel at room temperature with a storage modulus of ~11 Pa at 1 rad s^{-1} (Fig. S1;† liquid to gel transition can be observed as cooled below 40 °C).

Electrical recordings

Two ball-end silver–silver chloride (Ag/AgCl) wire-type electrodes (120 μm dia.) are mounted on separate micromanipulators to allow independent manipulation of droplet positions and to serve as electrodes for applying voltage and measuring current across the DIB. Before placing the electrodes under the bulk solvent, the ball-end tips (~300 μm dia.) are coated with molten 1–2% agarose (Sigma Aldrich) to enhance droplet adhesion to the probes. Aqueous droplets containing DPhPC liposomes are then placed on each agarose-coated electrode tip within the bulk phase and left undisturbed for the required incubation period to achieve sufficient lipid monolayer assembly. After this mandatory incubation period, droplets are brought into contact by manipulating the droplet positions to form a DIB.

Electrical properties such as membrane resistance, rupture potential, specific capacitance, electrowetting response between adjoined droplets, and voltage-dependent ion channel gating are investigated *via* electrical measurements. Voltage is applied to DIBs and the resulting currents are measured at a sampling frequency of 2 kHz (unless noted otherwise) using an Axopatch 200B single channel patch clamp amplifier and Digidata 1440A data acquisition system controlled by AxoScope software (Molecular Devices). Membrane resistance is determined from the reciprocal of the slope of average current *versus* DC voltage measurements made in 25 mV increments from −150 mV to +150 mV (Fig. S2†). The rupture potential is defined by the DC voltage at which the bilayer ruptures and droplets coalesce. Nominal bilayer capacitance is measured by analyzing the square waveform current induced from applying a continuous 10 mV, 10 Hz triangular waveform. Specific capacitance of the membrane is determined by a technique described elsewhere.[15,26] Alamethicin ion-channel gating is recorded by applying a DC voltage above 70 mV and recording the resultant current at a sampling frequency of 10 kHz.

DIB durability

The durability of each DIB system is quantified by performing vibration experiments in which the DIB embodiments are vibrated horizontally in a direction perpendicular to the bilayer. The DIB systems are vibrated at multiple frequencies ranging from 10 Hz to 60 Hz and varying displacements in order to impose a range of accelerations. An L-shaped stage made of aluminum (see Fig. S3.A†) is fixed to an electromagnetic shaker (Brüel & Kjær 4810), which is

mounted firmly on a vibration isolation table. The shaker is driven by a sinusoidal voltage waveform output by a custom LabVIEW program. A KEPCO BOP 20-5D power amplifier is used to deliver the required current to the shaker. An accelerometer (PCB Piezoelectronics; model 480E09) is mounted on the aluminum stage in the direction of the vibration to measure the amount of applied acceleration. The voltage output from the piezoelectric sensor is digitized using the Digidata 1440A and the acceleration is computed using AxoScope software. In addition to the vibration experiment, the durability of the liquid-in-gel DIB is also investigated by performing a simple drop experiment in which a PDMS substrate containing a liquid-in-gel DIB is dropped from varying heights onto a table until the bilayer ruptures and the droplets coalesce. Visual detection of droplet coalescence is aided by adding water-soluble food coloring into one of the two droplets.

Results and discussion

Formation and characterization of liquid-in-gel DIBs

SEBS triblock copolymer consists of glassy polystyrene (PS) endblocks and a rubbery poly(ethylene-butylene) (PEB) midblock. The SEBS (Kraton G1650) used in this work is 31% polystyrene with a fractional molecular weight of 27 900 g mol^{-1} and 69% poly(ethylene-butylene) with a fractional molecular weight of 62 100 g mol^{-1}.[27] When mixed with a midblock-selective solvent such as hexadecane at elevated temperature (>100 °C), a clear homogenous solution is obtained in which the polymer molecules exist in disordered state. When cooled below the order–disorder transition temperature (~45 °C; see Fig. S1.A–C† for rheology data), SEBS triblock molecules microphase segregate to form a weak gel in which the polymers are present in an ordered state. During this microphase segregation (order–disorder transition), the PS-endblocks that are insoluble in hexadecane cluster together to form nanoscopic micelle cores, while the soluble PEB-midblocks either loop into the same PS core or span between adjacent PS cores in a hexadecane-filled inter-micellar space to form a continuous organic gel.[27–29] At high concentrations of SEBS/hexadecane (≥50 mg ml^{-1}), the organogel shows flexibility and retains its shape (see Fig. S1.D†); at 10 mg ml^{-1} used herein for encapsulation, the gel does not hold shape very well and is considerably more viscous. While this process requires heating to ~45 °C, we note that this temperature is below the denaturation temperature of many peptides and proteins, including that for alamethicin, α-hemolysin, and bacteriorhodopsin, which denature above 65 °C,[30–32] which have been frequently incorporated into DIBs to provide stimuli-responsive functionality or enhance transport. Therefore, this material should be compatible with many types of functional biomolecules.

It has been shown previously[24] that connecting aqueous droplets containing DPhPC liposomes after incubating them in hexadecane for 5 minutes at room temperature yields DIBs nearly 100% of the time. For the same sized droplets placed under molten SEBS/hexadecane at 50 °C, we observe that droplets in contact spontaneously form a stable adhesive interface at a rate of *ca.* 80% (n = 40 trials) when they are joined after 2–3 minutes for monolayer assembly. In contrast, droplet coalescence occurs when the incubation time is shorter than 1 minute. Yet, longer incubation time does not improve the success rate of DIB formation. In fact, connecting droplets after more than 5 minutes of incubation results in neither coalescence nor spontaneous bilayer thinning. The observation that droplets simply remain separate instead of forming an adhesive connection suggests either that SEBS triblocks interact with the lipid monolayers or multiple layers of lipids assemble at the oil–water interface,[33,34] both which make bilayer formation unfavorable. Compared to assembly of lipids in the absence of SEBS and at room temperature, we attribute the shorter incubation time required for droplets placed in molten organogel *versus* hexadecane to the increased rate of monolayer assembly expected at an elevated temperature.[34] DIBs formed in molten gel are found to be stable for several minutes. However, we observe that usually within 10 minutes, the droplet pair fall off the suspended wire-type electrodes, which is likely due to accelerated droplet shrinkage at an elevated temperature which we believe leads to a decreased interfacial tension and poorer adhesion to the electrodes caused by tighter packing of lipids in the monolayer. Cooling the system to room temperature causes the organic phase to gel. Similar to the use of microfluidic methods for DIB encapsulation,[35,36] this transformation restrains the droplets in place and preserves electrical contact with the droplets without disturbing the bilayer formed at the interface. Once cooled, the bilayer is found to be stable for a minimum of 12 hours, similar to that observed for conventional DIB.[5] Fig. 2 shows bright-field images of a DIB in molten and cooled SEBS gel. Unlike prior studies which yielded membranes that were sandwiched between hydrogels,[37,38] this approach results in a liquid-supported bilayer between organogel-encased droplets. The system can also be reheated to re-melt the SEBS gel without rupturing the bilayer (Fig. S4.A and C†). Attempts to assemble DIBs in higher concentration SEBS/hexadecane (>30 mg ml^{-1}) requires heating the system to higher temperatures (>60 °C) which lowered the success rate for DIB formation.

An important aspect of this work is to determine if SEBS copolymers present in the external medium can stabilize the

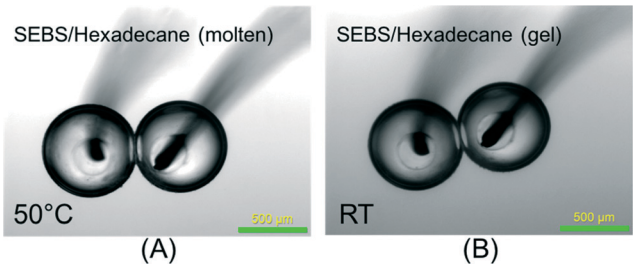

Fig. 2 Micrographs of a DIB formed in molten 10 mg ml^{-1} SEBS-gel (A) and cooled to room temperature (B). Scale bar represents 500 μm.

interface between droplets in the absence of lipids. As a control experiment, aqueous droplets devoid of lipids are placed in molten SEBS/hexadecane solution and brought into contact after 20 minutes of incubation. These experiments (n = 5) repeatedly show that droplets coalesce when placed in contact under molten SEBS/hexadecane without lipids present. This finding affirms prior interfacial tension measurements,[39] which showed that, despite being amphiphilic, these polymer molecules do not self-assemble at an oil–water interface like lipid molecules to form a monolayer. As a result, we would not expect, nor do we find, that SEBS molecules can stabilize the interface between two droplets.

These first two experiments allow us to conclude that the lipids, and not the polymer molecules, comprise the monolayer surrounding each droplet. However, an open question is whether any polymer molecules present in the bulk are trapped in the interface upon formation of the membrane between droplets. To determine if SEBS polymers are being retained, we measure the area-normalized specific capacitance, C_m, given by

$$C_m \equiv \frac{C}{A} = \frac{\varepsilon_0 \varepsilon_r}{d}, \quad (1)$$

where C and A are the nominal capacitance and area of the membrane, respectively, ε_0 is the dielectric permittivity of vacuum, and ε_r and d are the relative dielectric permittivity and thickness of the hydrophobic region of the membrane, respectively. C_m is determined experimentally by measuring nominal membrane capacitance, C, and area, A, of a DIB while sequentially varying the bilayer size *via* step-wise manipulation of the relative positions of droplets using the electrodes, as described elsewhere.[24,26,40] By measuring C_m and assuming a value for ε_r (2.2 is used herein),[41] we can thus calculate values of d for bilayers formed in the presence and absence of SEBS. Unfortunately, this C_m-measurement technique is inapplicable for the liquid-in-gel system at room temperature since the positions of droplets are severely constrained in gel-encapsulated DIBs. Instead, C_m measurements are only performed on molten gel encapsulated DIBs (at 50 °C) for which droplet manipulation is not inhibited by solidified organogel.

Specific capacitance, C_m of liquid-in-liquid DPhPC DIBs in hexadecane is found to be 0.75 ± 0.07 μF cm^{-2} (Table 1). Using the same measurement technique, Taylor, *et al.* recently reported C_m values of 0.708 ± 0.02 μF cm^{-2} for DPhPC bilayers formed in hexadecane at 50 °C.[15] Note that the reduced C_m at higher temperature is due to the increase in the amount of hexadecane present in the bilayer region.[42] In comparison, the interface formed between aqueous droplets encapsulated in molten SEBS-gel at 50 °C is found to have a specific capacitance of 0.72 ± 0.05 μF cm^{-2}, which is not significantly different ($t(10)$ = 0.542, p = 0.599) from that of liquid-in-liquid DIBs formed in hexadecane at the same temperature. Using eqn (1), we see that these values for C_m yield estimates of *ca.* 2.6–2.7 nm for the hydrophobic thickness of the membrane in the presence and absence of SEBS in the surrounding medium at 50 °C. These statistically similar values, which match well with the literature, thus prove that the interface between droplets is that of a single lipid bilayer and that it does not contain any trapped SEBS in the molten state.[26,40]

It is well established that small hydrophobic molecules, like those of *n*-alkanes of equal or lesser length than that of the phospholipid acyl chains,[43–45] can remain trapped in a planar lipid bilayer. More specifically, the presence of solvent in a bilayer can increase membrane thickness (and thus decrease specific capacitance) as well as increase the lateral tension of bilayer due to increasing spacing between neighboring lipids.[26,40] In DIBs, where the volume of the aqueous phase is conserved, increasing the bilayer tension relative to that of the monolayers results in a decrease in the area of adhesion between adhesive droplets. For example, a DIB in decane (142 g mol^{-1}) has more solvent in the bilayer region leading to higher bilayer tension and a smaller bilayer area than is obtained with hexadecane (226 g mol^{-1}) as the oil.[40] Conversely, a larger-molecule solvent such as squalene (411 g mol^{-1}) yields a more "solvent-free" DIB with a larger contact area due to the poorer solubility of the oil in the acyl chains of the monolayers.[25,46] The SEBS copolymers used in this work are significantly larger (90 kg mol^{-1}) than solvents such as hexadecane and squalene used to form DIBs to-date. Therefore, SEBS molecules are expected, and found (at 50 °C), to be completely excluded from the hydrophobic region of the bilayer, but not necessarily change how much hexadecane remains in the membrane (<10% for DPhPC bilayers at RT[26]). As a result, the estimated hydrophobic thicknesses of bilayers formed in liquid-in-gel system in the molten state are very similar to those of liquid-in-liquid DIBs formed in hexadecane alone.

Achieving a polymer-free DIB in the molten state for the organogel mixture also means that it is highly unlikely for

Table 1 Electrical and physical properties of liquid-in-liquid and liquid-in-gel DIBs

	Liquid-in-liquid	Liquid-in-gel	
Property	RT	RT	50 °C
Specific capacitance, C_m (μF cm^{-2})	0.75 ± 0.07	—	0.72 ± 0.05
Estimated bilayer thickness, d (nm)	2.6 ± 0.2	—	2.7 ± 0.2
Resistance (GΩ)	218.9 ± 72.3	257.6 ± 68.9	99.3 ± 69.8
Rupture potential (mV)	219 ± 24	196 ± 34	161 ± 32
Electro-wetting constant, α (V^{-2})	11.82 ± 1.6	8.2 ± 2.2	18.7 ± 3.5

polymer species to enter the membrane upon cooling to the gelled state, where triblocks integrate into a gel network that has an even higher molecular weight. Specifically, at room temperature, the interconnected polystyrene cores in this gel matrix are found to be about 7 nm wide,[27] which makes it highly unlikely for SEBS polymers or aggregates to enter the hydrophobic region of the bilayer. Note that the slight reduction in nominal membrane capacitance during cooling process (Fig. S4.B†) is due to the reduction in the amount of hexadecane trapped in the bilayer region.[15] This further supports our claim that polymer molecules do not incorporate into membrane upon cooling (or reheating).

The electrical properties of liquid-in-liquid DIBs and liquid-in-gel DPhPC DIBs are also compared in Table 1. A high bilayer resistance is indicative of a desirable leak-free membrane. Rupture potential gives information regarding the practical voltage range that can be applied to the bilayer before complete breakdown of bilayer takes place, causing droplet coalescence. Resistance and bilayer rupture potential of liquid-in-gel DIBs (257 ± 68.9 GΩ; 196 ± 34 mV) are found to be not significantly different from that of liquid-in-liquid DIBs (218.9 ± 72.3 GΩ; 219 ± 24 mV); unpaired *t*-test values for resistance ($t(6) = 0.77$, $p = 0.468$) and rupture potential ($t(6) = 1.105$, $p = 0.311$) further prove that these membrane properties are statistically similar (*i.e.*, $p > 0.05$). However, the electrical resistance of liquid-in-molten gel DIBs are found to be significantly lower than liquid-in-gel DIBs; a calculated *t*-test value of $t(6) = 3.228$, $p = 0.018$ is obtained, which shows that the membrane resistance is statistically higher once the system is cooled. A decrease in bilayer resistance at elevated temperatures has been reported in previous works.[15]

Electrowetting responses to assess gel confinement of DIBs

Application of a voltage across a lipid bilayer reduces its lateral tension due to the electrowetting of the dielectric between droplets, which increases the contact angle between the pair and the interfacial area, due to the conservation of droplet volume.[12,47] This increase in bilayer area causes nominal membrane capacitance to increase with the magnitude of the applied voltage. In oil-rich membranes, an applied voltage can also increase the capacitance per unit area of a membrane as a result electrostriction that reduces the hydrophobic thickness of the bilayer. However, this increase in specific capacitance was found to be relatively insignificant (<1.5% for ±100 mV) for DPhPC bilayers formed in hexadecane.[26] Therefore, the nominal capacitance of a DIB in hexadecane is expected to increase as given by

$$C(V) = C_0(1 + \alpha V^2) \quad (2)$$

where, $C(V)$ is the bilayer capacitance at applied voltage, V, C_0 is the capacitance at zero volts, and α is the electrowetting proportionality constant with a value ≥ 0.[12,40,48]

We aim to qualitatively evaluate differences in DIB confinement caused by the organogel by comparing the amount by which the membrane can increase in area due to electrowetting. The electrowetting responses of DIBs formed in liquid and in gel are quantified by measuring nominal bilayer capacitance at varying DC biases from 0 to +150 mV. Fig. 3A shows the normalized capacitance, $(C(V) - C_0)/C_0$, *versus* the square of the voltage for representative measurements on these DIB systems. In this representation, we see that all conditions exhibit a fairly linear relationship between normalized capacitance and voltage squared, where the slope of each represents α.

Liquid-in-liquid DIBs whose boundaries are not constrained by the surrounding medium exhibit an average α value of 11.82 ± 1.6 V^{-2} at RT and 17.02 ± 3.0 V^{-2} at 50 °C. Liquid-in-molten gel DIBs are found to produce a comparable α value of about 18.7 ± 3.5 V^{-2}. Liquid-in-gel DIBs, on the other hand, display a reduced α value of 8.2 ± 2.2 V^{-2}, suggesting that the gel imposes a geometric constraint on the bilayer. Fig. 3B shows microscopic images of bilayers and the measured bilayer size under 0 mV and +150 mV applied voltage for liquid-in-gel system at molten state (50 °C) and at gel state (room temperature). The difference in bilayer size between the molten and gel states at 0 mV is due to a small drift in the relative electrode positions during the cooling process. Nevertheless, the constriction of electrowetting-induced bilayer growth at gelled state is evident from the difference between the measured bilayer sizes at 150 mV: a ~36 μm increase in equivalent bilayer diameter for molten state as opposed to ~19 μm for gel state. Similar magnitude of bilayer growth was reported for liquid-in-liquid DIBs in prior literature.[12] While the reduced α value can be attributed to the constrained annulus, it is important to note that α is not zero. This finding could be due to: a) a thin layer of liquid hexadecane separating the water droplets from the gel, allowing for some bilayer expansion, b) the low stiffness of soft gel, which allows electrowetting to compress the organogel in the annulus region and allow bilayer expansion, or c) combination of both a & b (see ESI† for additional information).

Verification of functional properties of membrane-bound peptides

Alamethicin is a voltage-activated, pore-forming peptide that forms ion channels in fluid lipid bilayers.[49] To further validate that the interface between gel-encapsulated droplets is in fact a lipid bilayer and not a polymeric interface, we added 1 μM alamethicin to the liposome solutions that comprise the droplets. Fig. 4 shows the ion currents through alamethicin channels contained in a liquid-in-gel DPhPC bilayer at 25 °C in response to an applied voltage of +175 mV. The corresponding histogram of conductance levels (*i.e.* current divided by applied voltage; unit: pS) shows multiple discrete conductance levels and sub-conductance levels that are characteristic of alamethicin channels in a fluid lipid bilayer.[15,50] In comparison, measurements of alamethicin gating in a DIB surrounded by molten gel at 50 °C shows shorter

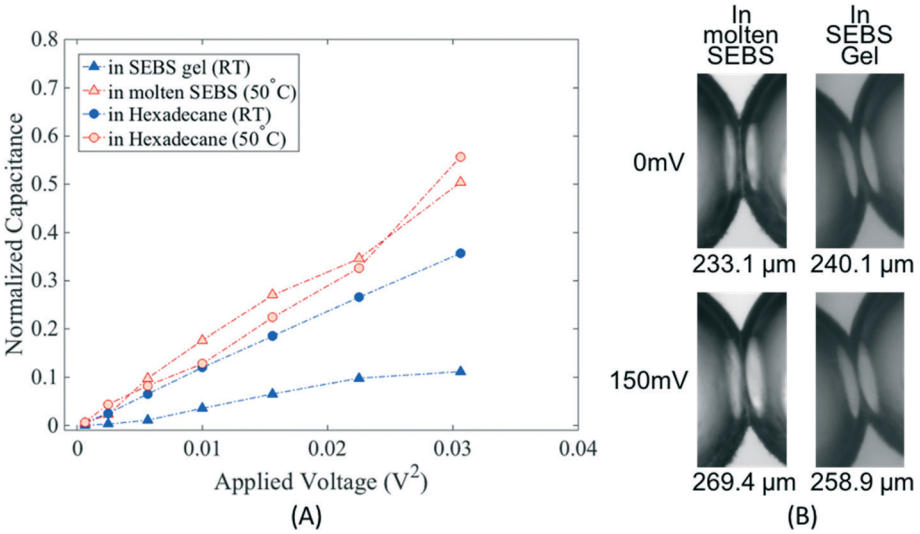

Fig. 3 Electrowetting behavior of DIBs in SEBS-gel and in hexadecane at RT (blue) and 50 °C (red); the increase in capacitance of bilayer with applied voltage is plotted according to eqn (1) (A). (B) Bright-field microscopic images of a single DIB at 0 and 150 mV applied voltage in molten and gelled SEBS.

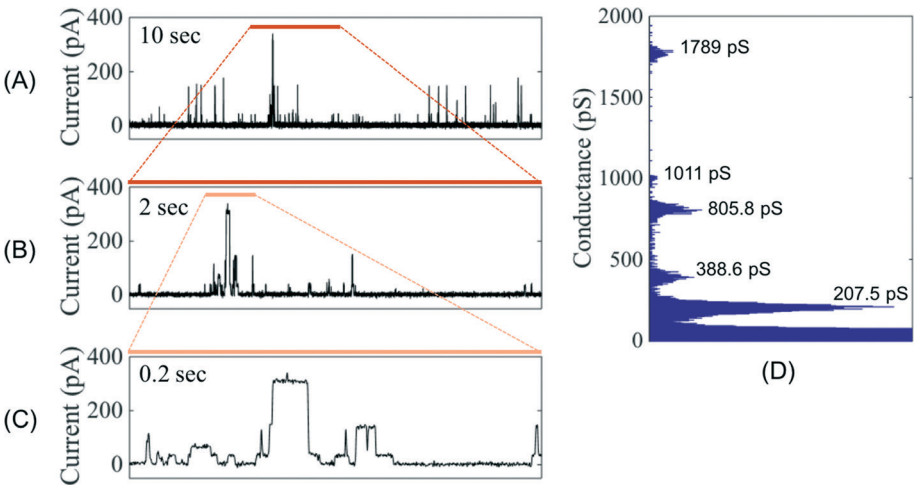

Fig. 4 Single-channel alamethicin recording at +175 mV applied voltage at room temperature (A–C). Single-channel recordings at 50 °C are provided in Fig. S6.† (D) Histogram of conductance levels corresponding to trace in A. Normalized conductance ratios with respect to the first conductance level are found to be 1 : 2 (1st to 2nd level), 1 : 4 (1st to 3rd), 1 : 5 (1st to 4th) & 1 : 9 (1st to 5th).

channel dwell times ("flicker") when compared to its activity at room temperature (Fig. S6†).[15,51] This channel activity at both temperatures confirms that the membrane retains its fluid environment across the temperature range, which enables channel insertion, and, at least for alamethicin, we observe that the heating required to assemble the DIB within a molten gel does not prevent functional channel activity upon cooling to room temperature.

Vibration experiments to quantify durability of DIBs

Two modes of DIB failure are observed during the vibration experiments: droplet separation and droplet coalescence induced by bilayer rupture. In Fig. 5A, the data from these experiments are presented in a way that shows, *versus* frequency, the applied acceleration that induces loss of the bilayer. Note that for liquid-in-liquid DIBs, this value of acceleration does not account for acceleration amplification due to droplet motions relative to the substrate, as described previously.[21] Nonetheless, similar to this prior study,[21] we find that liquid-in-liquid DIBs (○) exhibit droplet separation at a comparable average of 2.1 ± 1.0 g (n = 14) across the frequency range from 35 to 60 Hz. In contrast, liquid-in-gel DIBs shaken at maximum achievable accelerations below 50 Hz (due to the power limitation of the shaker[52]) did not separate or rupture (▲). However, when accelerated at 50 Hz and 60 Hz, liquid-in-gel DIBs (△) ruptured at an average acceleration of 6.0 ± 1.9 g (n = 9) (Fig. 5B). An unpaired t-test result of $t(11) = 2.68$, $p = 0.0216$ performed on this subset population (50 & 60 Hz) of bilayer failure accelerations thus confirms that the liquid-in-gel DIBs rupture at a significantly higher applied acceleration. Similar modes of failure were reported

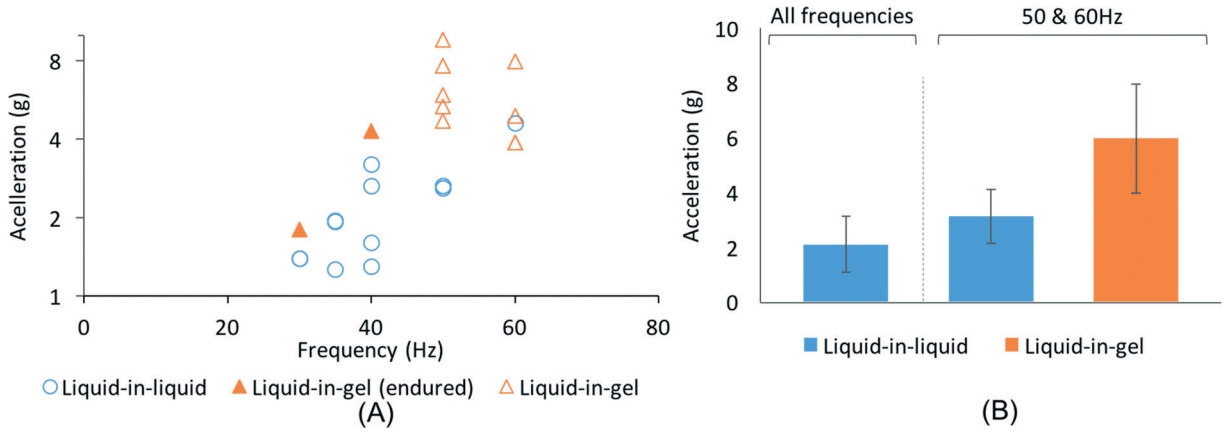

Fig. 5 Measured values of applied acceleration that triggered bilayer failure for liquid-in-liquid and liquid-in-gel DIBs, plotted with respect to excitation frequency (A). Bar graph comparing the average accelerations at failure across all frequencies (n = 14; left), and at 50 & 60 Hz ($n \geq 4$; right) (B). Error bars represent ± one standard deviation.

for un-encapsulated and PDMS-encapsulated DIBs.[21] Across the frequencies tested herein, SEBS-encapsulated DIBs are found to be comparably durable to PDMS-encapsulated DIBs reported previously by Sarles and Leo.[21]

In addition to the critical accelerations that can be withstood, this experiment again shows that the amount of confinement surrounding the adhesive droplets affects the mode of failure. We observe that droplet pairs placed in liquid hexadecane are not constrained in their relative positions due to the absence of contact to solid supports on all sides, except beneath the droplets. This lack of confinement allows droplets to both deform from their static spherical shapes and move relative to one another, leading to droplet separation, and thus bilayer unzipping, upon vibration. Droplet deformation could also lead to an increase in monolayer tension (due to transient fluctuations in surface area), which may also lead to bilayer unzipping according to the force balance equation described by Young–Dupré.[13] SEBS-encapsulated droplet pairs, on the other hand, are surrounded by gel (in all directions except for the thin region beneath the droplets) that highly constrains droplet deformation and provides structural support to the droplet pair as a whole. Therefore, when vibrated, due to the minimized droplet deformation and relative motion between the droplets, the droplets do not separate and thus, can withstand higher levels of acceleration because of the additional support when compared to liquid-in-liquid DIBs. However, at high accelerations (>6 g) the bilayer experiences higher magnitude forces and the bilayer fails, causing the droplets to coalesce. Sarles and Leo reported droplet separation as the mode of failure even for encapsulated DIBs (no electrodes),[21] which is possibly due to the amount of bulk liquid hexadecane that surrounds the aqueous droplets and the extent to which the droplets are still free to move in the compartments.

Nevertheless, with bilayers that can withstand nearly 3× higher applied acceleration, liquid-in-gel DIBs offer a more robust and more portable embodiment than conventional DIBs. Unlike liquid-in-liquid DIB devices, liquid-in-gel DIB devices eliminate spillage of bulk organic phase thus improving handling and portability of the device—a feature desired in many droplet-based applications including DIBs. A liquid-in-gel DIB formed in a PDMS substrate was subjected to a simple drop experiment and is found to withstand a ~0.5 foot drop with an estimated acceleration of ~12 g felt at impact (see Movie S1†). In order to demonstrate its improved handling, a liquid-in-gel DIB is formed on a flexible substrate (Dynaflex G6713) as shown in Fig. 6A. The rupture of the bilayer is monitored visually by using droplets containing water-soluble food coloring. Once the organogel is cooled to room temperature, the substrate is subjected to simple handling such as moving, lifting, flipping upside down, and bending, and the DIB is found to be preserved. Such manipulations of a substrate containing a liquid DIB would have resulted in DIB failure and droplet and oil spillage.

Developing a portable DIB system that can be used for long-term sensitive measurements must also consider taking preventive measures from possible contaminants such as dust particles and other aqueous droplets. Fig. 6B shows a flexible substrate with a functional DIB being submerged into water, demonstrating the ability of the SEBS-gel to act as a physical barrier to effectively isolate the DIB assembly from the surrounding environment and improving useful longevity (>24 hours) of sensitive experiments in settings outside of laboratories. In addition, because SEBS encapsulation simply replaces the oil phase and does not require a specific substrate, we envision this approach could also help protect large DIB arrays and may even facilitate the fabrication of multilayered droplet assemblies.

Fig. 6C and Movie S2† demonstrates force transmission through the gel by applying force externally to a flexible substrate that contains the DIB. Deformation of droplets and slight increase in bilayer size can be seen when the substrate is subjected to a force from the direction depicted by the arrow mark. Such indirect force transmission capability, in contrast to direct application of force as demonstrated by Najem *et al.*,[13,53] could be used for activation of mechanosensitive

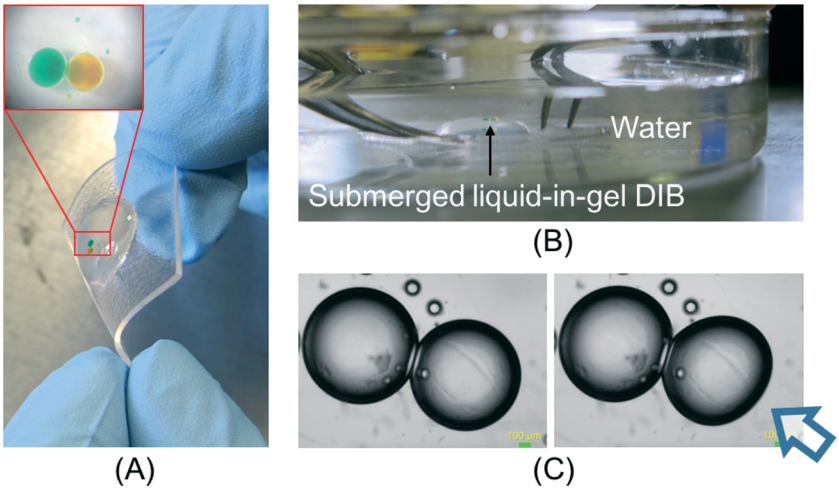

Fig. 6 Demonstrating the portability and improved handling of SEBS-encapsulated DIBs: A) DIB formed on a flexible, open substrate, and B) DIB submerged under water testifying physical shielding from environment. C) Application of indirect force to perturb the DIB.

ion channels like MscL by external forces, potentially eliminating the need for a complex droplet-shaking setup and yielding new types of membrane-based materials for cell-inspired transduction.

In summary, liquid-in-gel DIBs in a polymer-based organogel encapsulation were assembled and found to exhibit improved durability and portability at room temperature when compared to conventional liquid-in-liquid DIBs. SEBS polymer molecules are found to not assemble themselves or interfere with the lipid self-assembly process that forms a monolayer at the oil–water interface. We also found that these polymer molecules are excluded from the bilayer region during the thinning process, yielding a polymer-free lipid bilayer that has statistically similar electrical and structural properties to that of conventional liquid-in-liquid DIBs. The fact that DPhPC bilayers (which do not exhibit a thermotropic transition in the temperature range tested[54]) can withstand multiple heating (50 °C) and cooling (20 °C) cycles required to melt and solidify the gel indicates that this approach preserves the ability to add, remove, and rearrange droplets in a DIB network. This temperature range should also be suitable for a wide-variety of phospholipids, surfactants, and other biomolecules that are typically used and studied in model membranes. Unlike a liquid solvent, using a gel-phase material to encapsulate droplet interface bilayers facilitates force transmission to the bilayers through the surrounding medium, enabling membrane-based materials that could be used to sense applied force, stretch, and compression.

Furthermore, we believe that this approach could be integrated with hydrogel-based DIB systems, in which one or both the participating aqueous droplets are replaced with hydrogel (agarose or PEG),[38,55,56] to yield gel-in-gel DIB assemblies that could be even more mechanically stable. Our preliminary experiments show that SEBS does not affect gel-in-gel bilayer formation. Alternate to a SEBS/hexadecane organogel, SEBS/mineral oil organogel and pure paraffin wax without polymer can also be used to achieve gel- and wax-encapsulated DIBs following the same procedure of DIB formation in the molten organic phase (Fig. S7†). Specific advantages of the organogel material *versus* paraffin wax include maintaining a transparent encapsulation material upon gelling and a reduced volume shrinkage during the phase transition that helps maintain the bilayer between droplets. Development of such lipid membrane based soft-materials that are more portable and durable enables researchers to design wider range of useful bioinspired membrane-based devices. More broadly, we note that the approach demonstrated here can also be used for solidifying the continuous organic phase in droplet-based emulsions assembled in both closed microfluidic systems[57,58] and open surface microfluidic systems,[59,60] where, in particular, the use of a solidifying external phase can be used to stabilize droplet positions and enhance durability and portability.

Acknowledgements

The authors acknowledge funding from the Air Force Office of Scientific Research Basic Research Initiative grant number: FA9550-12-1-0464. The authors also acknowledge Dr. Yangyang Wang of Oak Ridge National laboratory for his assistance with rheological characterization of SEBS organogels.

References

1 P. Kongsuphol, K. B. Fang and Z. Ding, *Sens. Actuators, B*, 2013, **185**, 530–542.
2 M. Zagnoni, *Lab Chip*, 2012, **12**, 1026–1039.
3 Y.-x. Shen, P. O. Saboe, I. T. Sines, M. Erbakan and M. Kumar, *J. Membr. Sci.*, 2014, **454**, 359–381.
4 K. Funakoshi, H. Suzuki and S. Takeuchi, *Anal. Chem.*, 2006, **78**, 8169–8174.
5 H. Bayley, B. Cronin, A. Heron, M. A. Holden, W. L. Hwang, R. Syeda, J. Thompson and M. Wallace, *Mol. BioSyst.*, 2008, **4**, 1191–1208.

6 W. L. Hwang, M. A. Holden, S. White and H. Bayley, *J. Am. Chem. Soc.*, 2007, **129**, 11854–11864.
7 M. A. Holden, D. Needham and H. Bayley, *J. Am. Chem. Soc.*, 2007, **129**, 8650–8655.
8 G. Villar, A. D. Graham and H. Bayley, *Science*, 2013, **340**, 48–52.
9 N. Tamaddoni, E. C. Freeman and S. A. Sarles, *Smart Mater. Struct.*, 2015, **24**, 065014.
10 P. J. Milianta, M. Muzzio, J. Denver, G. Cawley and S. Lee, *Langmuir*, 2015, **31**, 12187–12196.
11 S. A. Sarles and D. J. Leo, *J. Intell. Mater. Syst. Struct.*, 2009, **20**, 1233–1247.
12 S. Punnamaraju and A. J. Steckl, *Langmuir*, 2010, **27**, 618–626.
13 J. S. Najem, M. D. Dunlap, I. D. Rowe, E. C. Freeman, J. W. Grant, S. Sukharev and D. J. Leo, *Sci. Rep.*, 2015, **5**, 13726.
14 H. M. Barriga, P. Booth, S. Haylock, R. Bazin, R. H. Templer and O. Ces, *J. R. Soc., Interface*, 2014, **11**, 20140404.
15 G. J. Taylor and S. A. Sarles, *Langmuir*, 2015, **31**, 325–337.
16 T. Wauer, H. Gerlach, S. Mantri, J. Hill, H. Bayley and K. T. Sapra, *ACS Nano*, 2013, **8**, 771–779.
17 P. Mruetusatorn, J. B. Boreyko, G. A. Venkatesan, S. A. Sarles, D. G. Hayes and C. P. Collier, *Soft Matter*, 2014, **10**, 2530–2538.
18 S. Leptihn, O. K. Castell, B. Cronin, E.-H. Lee, L. C. M. Gross, D. P. Marshall, J. R. Thompson, M. Holden and M. I. Wallace, *Nat. Protoc.*, 2013, **8**, 1048–1057.
19 S.-H. Jung, S. Choi, Y.-R. Kim and T.-J. Jeon, *Bioprocess Biosyst. Eng.*, 2012, **35**, 241–246.
20 T.-J. Jeon, J. L. Poulos and J. J. Schmidt, *Lab Chip*, 2008, **8**, 1742–1744.
21 S. A. Sarles and D. J. Leo, *Lab Chip*, 2010, **10**, 710–717.
22 R. Kawano, Y. Tsuji, K. Kamiya, T. Kodama, T. Osaki, N. Miki and S. Takeuchi, *PLoS One*, 2014, **9**, e102427.
23 A. Laouini, C. Jaafar-Maalej, I. Limayem-Blouza, S. Sfar, C. Charcosset and H. Fessi, *J. Colloid Sci. Biotechnol.*, 2012, **1**, 147–168.
24 G. A. Venkatesan, J. Lee, A. B. Farimani, M. Heiranian, C. P. Collier, N. R. Aluru and S. A. Sarles, *Langmuir*, 2015, **31**, 12883–12893.
25 P. Poulin and J. Bibette, *Langmuir*, 1998, **14**, 6341–6343.
26 L. C. M. Gross, A. J. Heron, S. C. Baca and M. I. Wallace, *Langmuir*, 2011, **27**, 14335–14342.
27 T. Dürrschmidt and H. Hoffmann, *Colloid Polym. Sci.*, 2001, **279**, 1005–1012.
28 M. Sugimoto, K. Sakai, Y. Aoki, T. Taniguchi, K. Koyama and T. Ueda, *J. Polym. Sci., Part B: Polym. Phys.*, 2009, **47**, 955–965.
29 N. Mischenko, K. Reynders, K. Mortensen, R. Scherrenberg, F. Fontaine, R. Graulus and H. Reynaers, *Macromolecules*, 1994, **27**, 2345–2347.
30 G. A. Woolley and B. Wallace, *Biochemistry*, 1993, **32**, 9819–9825.
31 L. Bakás, M. P. Veiga, A. Soloaga, H. Ostolaza and F. M. Goñi, *Biochim. Biophys. Acta, Biomembr.*, 1998, **1368**, 225–234.
32 J. Müller, C. Münster and T. Salditt, *Biophys. J.*, 2000, **78**, 3208–3217.
33 S. Pautot, B. J. Frisken, J.-X. Cheng, X. S. Xie and D. A. Weitz, *Langmuir*, 2003, **19**, 10281–10287.
34 Y. A. Shchipunov and A. F. Kolpakov, *Adv. Colloid Interface Sci.*, 1991, **35**, 31–138.
35 Y. Bai, X. He, D. Liu, S. N. Patil, D. Bratton, A. Huebner, F. Hollfelder, C. Abell and W. T. S. Huck, *Lab Chip*, 2010, **10**, 1281–1285.
36 M. Zagnoni and J. M. Cooper, *Lab Chip*, 2010, **10**, 3069–3073.
37 X.-f. Kang, S. Cheley, A. C. Rice-Ficht and H. Bayley, *J. Am. Chem. Soc.*, 2007, **129**, 4701–4705.
38 T.-J. Jeon, N. Malmstadt and J. J. Schmidt, *J. Am. Chem. Soc.*, 2006, **128**, 42–43.
39 J.-J. Lin, I.-J. Cheng, C.-N. Chen and C.-C. Kwan, *Ind. Eng. Chem. Res.*, 2000, **39**, 65–71.
40 G. J. Taylor, G. A. Venkatesan, C. P. Collier and S. A. Sarles, *Soft Matter*, 2015, **11**, 7592–7605.
41 C. Karolis, H. G. Coster, T. C. Chilcott and K. D. Barrow, *Biochim. Biophys. Acta, Biomembr.*, 1998, **1368**, 247–255.
42 S. H. White, *Biophys. J.*, 1975, **15**, 95–117.
43 S. H. White, *Nature*, 1976, **262**, 421–422.
44 S. H. White, *Biophys. J.*, 1978, **23**, 337–347.
45 T. J. McIntosh, S. Simon and R. MacDonald, *Biochim. Biophys. Acta, Biomembr.*, 1980, **597**, 445–463.
46 P. Poulin, F. d. r. Nallet, B. Cabane and J. r. m. Bibette, *Phys. Rev. Lett.*, 1996, **77**, 3248–3251.
47 G. J. Taylor, G. A. Venkatesan, C. P. Collier and S. A. Sarles, *Soft Matter*, 2015, **11**, 7592–7605.
48 S. A. Sarles, J. D. W. Madden and D. J. Leo, *Soft Matter*, 2011, **7**, 4644–4653.
49 K. He, S. J. Ludtke, W. T. Heller and H. W. Huang, *Biophys. J.*, 1996, **71**, 2669–2679.
50 M. Eisenberg, J. E. Hall and C. Mead, *J. Membr. Biol.*, 1973, **14**, 143–176.
51 L. Bruner and J. Hall, *Biophys. J.*, 1983, **44**, 39.
52 Brüel & Kjær, Mini-shaker Type 4810 User Manual, http://www.bksv.com/Products/shakers-exciters/exciters/small-exciter-type-4810?tab=accessories&productoption=-4810-*–.
53 J. S. Najem, M. D. Dunlap, A. Yasmann, E. C. Freeman, J. W. Grant, S. Sukharev and D. J. Leo, *J. Visualized Exp.*, 2015, 53362, DOI: 10.3791/53362.
54 C. H. Hsieh, S. C. Sue, P. C. Lyu and W. G. Wu, *Biophys. J.*, 1997, **73**, 870–877.
55 S. A. Sarles, L. J. Stiltner, C. B. Williams and D. J. Leo, *ACS Appl. Mater. Interfaces*, 2010, **2**, 3654–3663.
56 J. R. Thompson, A. J. Heron, Y. Santoso and M. I. Wallace, *Nano Lett.*, 2007, **7**, 3875–3878.
57 R. B. Fair, *Microfluid. Nanofluid.*, 2007, **3**, 245–281.
58 D. Erickson and D. Li, *Anal. Chim. Acta*, 2004, **507**, 11–26.
59 J. B. Boreyko, G. Polizos, P. G. Datskos, S. A. Sarles and C. P. Collier, *Proc. Natl. Acad. Sci. U. S. A.*, 2014, **111**, 7588–7593.
60 M. R. R. de Planque, S. Aghdaei, T. Roose and H. Morgan, *ACS Nano*, 2011, **5**, 3599–3606.

